Available online at www.sciencedirect.com
SCIENCE DIRECT®
Journal of Molecular Graphics and Modelling 22 (2003) 11–21
Journal of Molecular Graphics and Modelling
www.elsevier.com/locate/JMGM

Insertion of X-ray structures of proteins in membranes

Frederic Basyn [a], Benoit Spies [a], Olivier Bouffioux [a], Annick Thomas [b], Robert Brasseur [a,*]

[a] *Centre de Biophysique Moléculaire Numérique, Faculté Agronomique, 2 Passage des déportés, FSAGX, 5030 Gembloux, Belgium*
[b] *INSERM Unité 410, Hôpital X. Bichat, 75018 Paris, France*

Received 17 October 2002; received in revised form 21 February 2003; accepted 21 February 2003

Abstract

Few structures of membrane proteins are known and their relationships with the membrane are unclear. In a previous report, 20 X-ray structures of transmembrane proteins were analyzed in silico for their orientation in a 36 Å-thick membrane [J. Mol. Graph. Model. 20 (2001) 235]. In this paper, we use the same approach to analyze how the insertion of the X-ray structures varies with the bilayer thickness. The protein structures are kept constant and, at each membrane thickness, the protein is allowed to tilt and rotate in order to accommodate at their best. The conditions are said to be optimal when the energy of insertion is minimal. The results show that most helix bundles require thicker membranes than porin barrels. Moreover, in a few instances, the ideal membrane thickness is unrealistic with respect to natural membranes supporting that the X-ray structure requires adaptation to stabilize in membrane. For instance, the squalene cyclase could adapt by bending the side chains of its ring of lysine and arginine in order to increase the hydrophobic surface in contact with membranes. We analyzed the distribution of amino acids in the water, interface and acyl chain layers of the membrane and compared with the literature.
© 2003 Elsevier Science Inc. All rights reserved.

Keywords: Membrane protein; X-ray structures; Insertion; Membrane thickness

1. Introduction

Integral membrane proteins are at the interface between the cytoplasm and the external or the intra-organelle media of cells. They mainly account for two structural classes: bundles of α-helices and β-barrels. Up to now, eukaryotic plasma and reticulum proteins are α-helical while β-barrels are found in the outer membrane of Gram-negative bacteria and in the mitochondria and chloroplast membranes. The interactions between the transmembrane segments of proteins and the acyl chains of lipids are important to minimize the contact area between hydrophobic regions of proteins and water [1,2]. They can be crucial for the function and the structure of membrane proteins [3].

Protein stability and activity could be regulated by the tilting and the association of membrane spans in order to avoid a hydrophobicity mismatch. For example, the activity of the Ca^{++} ATPase from the sarcoplasmic reticulum of skeletal muscle was found to vary with the orientation of the transmembrane segments [4]. The transition between a single- and a double-strand structures of the gramicidin A (gA) was shown to depend upon variations of membrane thickness [5].

Hydrophobic mismatches could be important in membrane processes where lipids and proteins interact. For instance, in the folding of some integral membrane proteins, a hydrophobicity mismatch was suggested to promote preferential protein–protein interactions [6,7]. Mismatch can also facilitate membrane destabilization and thus fusion processes [8].

It was also suggested that the intracellular targeting of membrane proteins partly results from a hydrophobicity mismatch. Newly synthesized membrane proteins are inserted into the endoplasmic reticulum. They are then targeted to another membrane: one of the polarity factors could be the length of the lipid acyl chain [9]. This is suggested for the cytochrome b5 since increasing the transmembrane span by five amino acids leads to the relocalization of the protein at the plasma membrane [10]. This was also proposed for UBC6 which is currently found in reticulum endoplasmic and is targeted to the golgi when the tail anchor is increased from 17 to 21 amino acids and to the plasma membrane when the tail is increased up to 26 amino acids [11].

Bacteria are special materials since they can modulate their membrane thickness according to the composition of the growth media. However, eukaryotic cell plasma membranes appear to be thicker than bacterial membranes [12].

Abbreviations: MHP, molecular hydrophobicity potential; IMP, integral membrane protein; IMPALA, IMP and lipid association

* Corresponding author. Tel.: +32-81-622521; fax: +32-81-622522.
E-mail address: brasseur.r@fsagx.ac.be (R. Brasseur).

1093-3263/03/$ – see front matter © 2003 Elsevier Science Inc. All rights reserved.
doi:10.1016/S1093-3263(03)00122-0

Two proteins with different lengths of hydrophobic fragments can be in the same membrane and vice versa, two proteins with the same hydrophobic length can be in different bilayers [1]. Fluctuation of the insertion of peptide segments was reported to depend upon the amino acid hydrophobicity and number. Leucine spans could be shorter than alanine ones. This supports that the global hydrophobicity can be more important than the span length per se [13]. Local changes are also obtained through the orientation of side chains. Two types of amino acids may be of special importance in that aspect: aromatic and charged residues.

A model of membrane called IMPALA has been developed in our laboratory and was previously used to study the insertion of peptides in membranes [14,15]. Since the IMPALA results nicely fitted experimental data [16,17], the procedure was also used to test the insertion of membrane proteins [18]. In IMPALA, the membrane is described as a three layers system corresponding to the polar heads of lipids, the acyl chains and the polar heads of lipids on the other side. The membrane properties are constant in, the *x*–*y* plane, parallel to the membrane surface and, vary with the *z*-axis that describes the membrane thickness; $z = 0$ at the membrane center. Two energy terms describe the interaction of the protein with the membrane, a hydrophobicity and a perturbation term. In this paper, we study how the membrane thickness affects the insertion of 20 proteins and analyze the amino acid distribution in the bilayer.

2. Computational methods

2.1. IMPALA

IMPALA describes the membrane as apolar layers, the water content of which varies from 1.0 (the water phase) to 0.0 (the acyl chain of lipids). The interaction of the protein and the membrane is described by adding two energy restraint terms to the usual energy description of the protein. Those empirical terms vary with *z*, the position along the membrane thickness and are set to describe: (1) the bilayer hydrophobicity, that pushes hydrophilic atoms out and hydrophobic ones in; and (2) the lipid perturbation as a function of the protein accessible surface [18]. In this analysis, the protein structure is the X-ray structure and remains the same along the test. Therefore, the only changes of energy are due to the restraint terms.

Hydrophobicity term:

$$E_{\text{int}} = -\sum_{i=1}^{N} S_{(i)} E_{\text{tr}(i)} C_{(z_i)}$$

where N is the total number of atoms, $S_{(i)}$ the accessible surface of atom i to solvent, $E_{\text{tr}(i)}$ its transfer energy by unit of accessible surface area and $C_{(z_i)}$ the value of $C_{(z)}$ at the position z_i of the atom i.

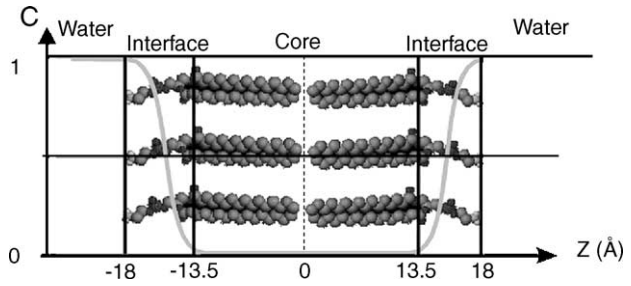

Fig. 1. Description of the IMPALA lipid–water interface simulation. The water content of the membrane is described by a function $C_{(z)}$ which varies along the *z*-axis normal to the membrane surface (plane *x*–*y*). The origin of *z* is at the center of the bilayer. $C_{(z)}$ is a symmetrical empirical function that is 1 from $-\infty$ to -18 Å (the water phase), varies from 1 to 0, -18 to -13.5 Å and 13.5 to 18 Å (lipid polar heads) and is null in the hydrocarbon core (from -13.5 to $+13.5$ Å).

Perturbation lipidic term:

$$E_{\text{lip}} = a_{\text{lip}} \sum_{i=1}^{N} S_{(i)} (1 - C_{(z_i)})$$

where a_{lip} is an empirical factor fixed to 0.018 and $C_{(z)}$ represent the empirical function describing the membrane properties, it is constant in the plane of the membrane (*x*- and *y*-axes) and varies along the bilayer thickness (*z*-axis) (Fig. 1) and more specifically at the lipid–water interface corresponding to the transition between the acyl chains of lipids (no water: hydrophobic core) and the outside medium (water: hydrophilic phase):

$$C_{(z)} = 1 - \frac{1}{1 + e^{\alpha(z - z_0)}}$$

The *z*-axis has its origin at the center of the bilayer (Fig. 1). $C_{(z)}$ varies from 0.0 (hydrophobic core) to 1.0 (hydrophilic phase); $\pm\infty < z < \pm 18$ Å are water phases, $\pm 18 < z < \pm 13.5$ Å are the polar heads of lipids, and $\pm 13.5 < z < 0$ Å are the acyl chains of lipids; α is a constant equal to 1.99 and z_0 correspond to the middle of heads polar ($(13.5 + 18)/2 = 15.75$ Å).

Changes of the sum of the restraints values are due to the tilt and rotation of the protein, to the displacement of the protein along the *z*-axis during a Monte Carlo procedure and, in this study, to the variation of the membrane thickness. Each Monte Carlo simulation was run as follows: temperature 25 °C, 10^5 steps, random rotation $\pm 5°$, random translation ± 4 Å. At the beginning of each run, the mass center of the molecule was set at the bilayer center. The most stable position(s) and orientation(s) were defined as corresponding to the lowest values of the restraints.

In the previous experiments, the membrane thickness was 36 Å distributed in the different layers as follows (water $= \infty$|lipid polar heads $= 4.5$ Å|two layers of acyl chains $= 27$ Å|lipid polar heads $= 4.5$ Å|water $= \infty$). In this study, the membrane thickness was varied from 20 to 60 Å by 1 Å step. The changes were all attributed to the acyl chains

(11–51 Å), the thickness of the lipid polar heads remaining constant.

At the optimal condition of protein insertion, each residue was mapped according to the position of its C_α in the membrane. The location was "phi" when the C_α was in water, "pho" when in the acyl chain layer, interface when it was at the lipid polar head level.

2.2. Pex-files

Two kinds of files were generated in this study. The Impala.pex2d-files are similar to the GF-Pex files previously described [19]: all amino acids of a protein are described, one line for each. The columns give different parameters of this amino acid in the protein three-dimensional (3D) structure such as the NH···OC H-bond length, its geometry and the partner residue, the secondary structure, the solvent-accessible surface, etc. In addition, the Impala.pex2d-files gives the position of each amino acid with respect to the membrane layers. Those Pex are available on the web site of the CBMN (http://www.fsagx.ac.be/bp/).

The second kind of file resumes the calculation made during the IMPALA simulation. Each line is a calculation step. Columns list the different parameters used and calculated during the simulation such as *x*, *y* and *z* values of the protein mass center, energy terms, tilt angles.

2.3. Molecular hydrophobicity potential (MHP) graph

MHP is a 3D plot of the hydrophobicity potential of a molecule in order to visualize its amphipathy. The isopotential surfaces of protein hydrophobicity were calculated by a cross-sectional computational method. A 1 Å mesh-grid plane was set to sweep across the molecule by steps of 1 Å. At each step, the sum of the hydrophobicity and hydrophilicity values at all the grid nodes were calculated. The hydrophobic and hydrophilic MHP surfaces were then drawn by joining the isopotential values. The brown zones correspond to hydrophobic regions and green zones to hydrophilic regions.

3. Results and discussion

We used the same panel of 20 membrane proteins as in the previous paper [18]. The membrane thickness was modified from 20 to 60 Å by 1 Å steps and the protein was allowed to tilt and rotate in order to find the optimal conditions of insertion. We postulated that the insertion is optimal when the restraints dictated by the interactions between the membrane and the protein are the lowest. For each membrane thickness we plotted the minimal energy restraint; it corresponded to a particular tilt and depth of insertion (Fig. 2). The plots show that two proteins: here, one α structure (KcSA, code PDB: 1BL8; [20]) and one β structure (code PDB: 1QJ9; [21]), have different profiles. The α protein is optimally inserted in a thicker membrane than the β protein (41 Å for the α protein as compared to 28 Å for the porin).

We further illustrated the results by adding the graphs of the inserted molecules at three different membrane thickness (Fig. 2). For the potassium channel protein KcSA (Fig. 2(A)) in a 41 Å membrane, there is a good match between the length of the acyl chains of lipids and the brown color corresponding to the hydrophobic surface of the protein. Hydrophilic regions, in green, are at the lipid interface and outside the bilayer, in water. The left insert shows how the protein stands in a shorter membrane: large hydrophobic area are outside the membrane and the protein tilt is not sufficient to decrease the hydrophobic surface in contact with water. The energy restraint value increases because of the contribution of the hydrophobic atoms in water. The right plot shows the protein in a thicker membrane: the protein stands perpendicular to the membrane surface, however, some hydrophilic patches are in contact with the hydrophobic core of membrane. This mainly results in an increase of the hydrophobicity term of the restraint because of the hydrophilic atoms in membrane.

For the porin OmpX (Fig. 2(B)), the lowest restraint corresponds to a bilayer thickness of 28–31 Å. In a thinner membrane, OmpX tends to tilt in order to increase the hydrophobic surface in contact with lipids. In a thicker membrane (right plot), hydrophilic patches are exposed to the membrane core.

These calculations enable us to estimate the optimal membrane thickness for the insertion of a rigid body structure of protein. Of course, because of this rigidity, the results do not presume of any intramolecular movement that the protein might undergo in order to adapt to the membrane thickness. Our calculations show that the membrane thickness can vary between 21 and 56 Å for α proteins and between 23 and 37 Å for β proteins with an average at 38 Å for α proteins and 29 Å for β proteins.

The optimal membrane thickness of each protein was compared to data from the literature when available (Table 1). Literature data are few but no major disagreement is noted. The thickness of plasma membranes was estimated to 40–50 Å by NMR experiments [22]. Molecular dynamics simulations of a bilayer composed of 1-palmitoyl-2-oleoyl-sn-glycero-3-phosphatidylcholine (POPC) covered with water molecules were run at different temperatures to ensure that the system was tested in the liquid–crystal phase [23]. The bilayer thickness was 58 Å for extended acyl chains and 46 Å in the fluid phase. This fits with the thickness in which a few structures optimally insert. However, several structures accommodate better in shorter bilayers. This is true for instance for the squalene hopene cyclase which optimally inserts in a 21 Å membrane. This suggests that either this proteins structurally adapts to fit in thicker membranes or migrates to very peculiar patches of membrane, or that it interacts with proteins rather than lipids.

Porins insert in the outer membranes of bacteria. Rahman et al. [12] looked for the lipid composition of a crude

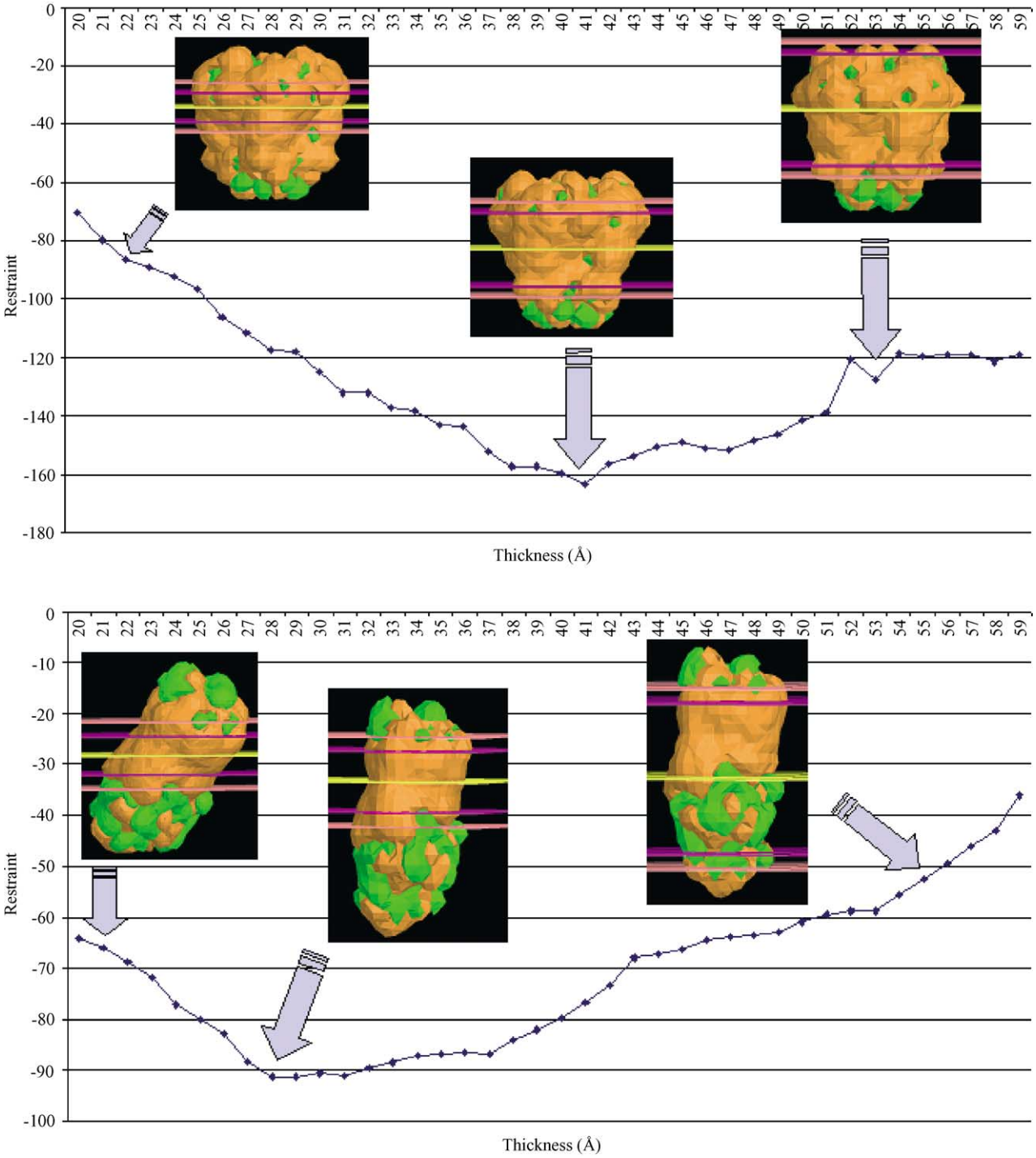

Fig. 2. The graphics plot the sum of the IMPALA energy restraints for different thickness of bilayer for: (A) an α protein, 1BL8: potassium channel protein (KcSA) [20]; and (B) a β protein, 1QJ9: OmpX [21]. The *x*-axis plots the total thickness of the bilayer and the *y*-axis plots the restraint value. Each point corresponds to the minimal restraint value (the best conformation) at that membrane thickness. The nadir of the plot is the best membrane thickness for the insertion of the RX structure. Three MHP's are plotted to illustrate the protein insertion in a, too thin, optimal, and too thick membrane, respectively.

extract of bacteria and found a high level of (^{14}C–^{12}C)-fatty acyl chains together with the occurrence of only few lipids with longer acyl chains. Therefore, membrane bacteria have shorter lipids than current eukaryotic plasma membranes [24]. Our data agree with this since porins are ideally inserted in shorter membranes than most eukaryotic proteins.

Considering each protein at its optimal condition of insertion, we then analyzed the distribution of amino acids in the three different membrane layers: water; interface; and

Table 1
Description of the proteins used in this study and comparison between IMPALA results and literature data

Name of the membrane protein	PDB code	Biological source	Optimal thickness (IMPALA simulations)	Theoretical/ experimental thickness	Corresponding Refs. to theoretical thickness
α Protein					
Photosynthetic reaction center	1AIG	*Rhodobacter sphaeroides*	38	40–45	[38]
Cytochrome Bc1	1BGY	*Bos taurus*	–	–	
Potassium channel protein (KcSA)	1BL8	*Streptomyces lividans*	41	34/35	[20,42]
Bacteriorhdopsin	1BRR	*Halobacterium salinarium*	37	47/50	[43,44]
Bacteriorhdopsin	1BRX	*Halobacterium Salinarium*	37	43.5/45	[45,46]
Prostaglandine H_2 synthase	1CQE	*Ovis aries*	45		
Fumarate reductase	1FUM	*Escherichia coli*	–	–	
Light harvesting complex II	1LGH	*Rhodospirillum molischianum*	56	52.5	[39]
MsCl (mechanosensitive ion channel)	1MSL	*Mycobacterium tuberculosis*	34	35	[40]
Cytochrome coxydase	1OCR	*Bos taurus*	–	–	
Squalene hopene cyclase	3SQC	*Alicyolobacillus aciddocaldarius*	21		
Rhodopsin	1F88	Not available	37		
β Protein					
OmpA (outer membrane protein A)	1BXW	*Escherichia coli*	37		
FepA (ferric enterobactin receptor)	1FEP	*Escherichia coli*	29		
OmpX	1QJ9	*Escherichia coli*	28		
Ompf	2OMF	*Escherichia coli*	38		
Sucrose specific porin	1AOS	*Salmonella typhimurium*	28	30–33	[47]
FhuA (ferric hydroxamate uptake receptor)	2FCP	*Escherichia coli*	31	34	[48]
Ompla (outer membrane phospholipase)	1QD6	*Escherichia coli*	27		[49]
OMPK36 (osmoporin)	1OSM	*Klebsiella pneumonia*	25		
Porin	1PRN	*Rhodopseudomonas blastica*	27		
Porin (crystal form B)	2POR	*Rhodobacter capsulatus*	23		
Malto porin	1AF6	*Escherichia coli*	29		

membrane core. We compared the amino acid composition using one major criteria: the amino acid accessibility. Amino acids are accessible to the solvent (lipid or water) when their accessible surface is more than 30% of their actual surface (100% is the residue surface in a Gly–X–Gly trimer as described by Creighton [25]).

In a representative panel of soluble proteins (bank of 131 PDB structures of proteins [19]), the solvent-accessible amino acids account for 40% of charged residues (D, E, K, R), 26% of polar ones (H, Q, N, S, T), 15% of hydrophobic residues (A, I, L, V), 7% of aromatic ones (F, W, Y), 4% of glycine and 5% of proline (Fig. 3(A)). In the membrane proteins, only 14% of the solvent-accessible residues are charged. This is three times less than in the soluble proteins. As expected, hydrophobic solvent-accessible residues are more frequent in membrane than in soluble proteins. This is especially true in the inner membrane layer where hydrophobic residues are three times more frequent than in PDB structures (Fig. 3(A)). Solvent-accessible aromatic and glycine residues are more frequent at all levels of membrane proteins (Fig. 3(A)). Conversely, there is little difference for proline.

The distribution of buried amino acids (solvent-accessible surface <30%) was also analyzed. The solvent-accessible and the buried residues of soluble proteins have different patterns: there is a large decrease of charged residues and a large increase of hydrophobic ones with burying. This is not true for membrane proteins where solvent-accessible and buried residues are similar. In conclusion, buried residues are similar for both types of proteins, and only the solvent-accessible residues in soluble and membrane proteins differ (Fig. 3(B)).

The distribution of amino acids along the membrane *z*-axis has also been analyzed (Fig. 4). For this, the optimal condition of the protein insertion was only taken into account, and the α and the β proteins were separated.

Charged residues: For the α proteins, positively charged residues (lysine and arginine) are frequent at the interface on the cytoplasmic side. Aspartic acid, but not glutamic acid, is frequent on the opposite extracellular side (Fig. 4). This is in agreement with the positive-inside rule of von Heijne [26] who postulated that cytoplasmic segments contain more positive charges than extracytoplasmic (periplasmic) ones. The rule does not seem to be true for β proteins: arginine, lysine and aspartic acid are more frequent outside the membrane, but the positively charged residues are more frequent on the extracellular side, and the aspartic residue more frequent on the cytoplasmic side. Glutamic acid is homogenously distributed between the two layers. Hence, in our set of β structures the von Heijne's rule is not true.

In the literature, the backbones of lysine and arginine were reported to be inserted deep into the bilayer, the side chains bending towards the aqueous phase and the charges protruding near the lipid phosphate group [27,28]. This is not checked in the present analysis, since the C_α of lysine and

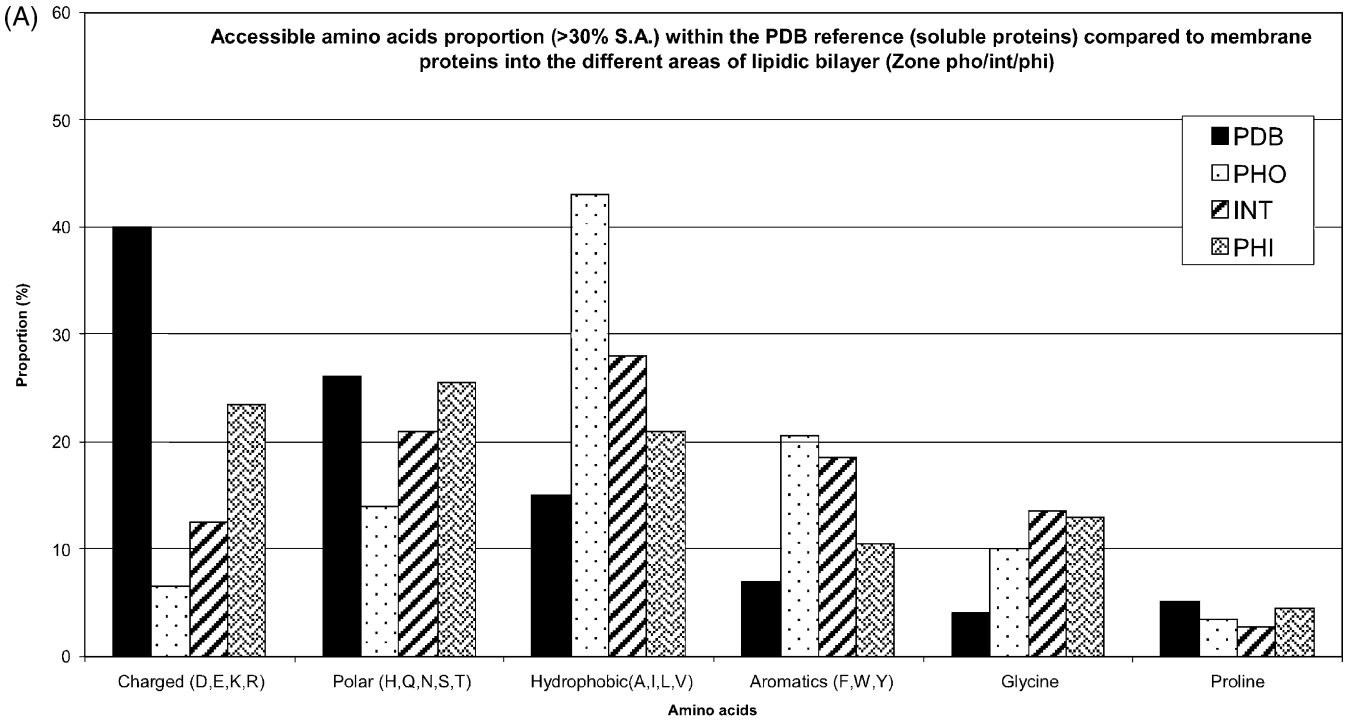

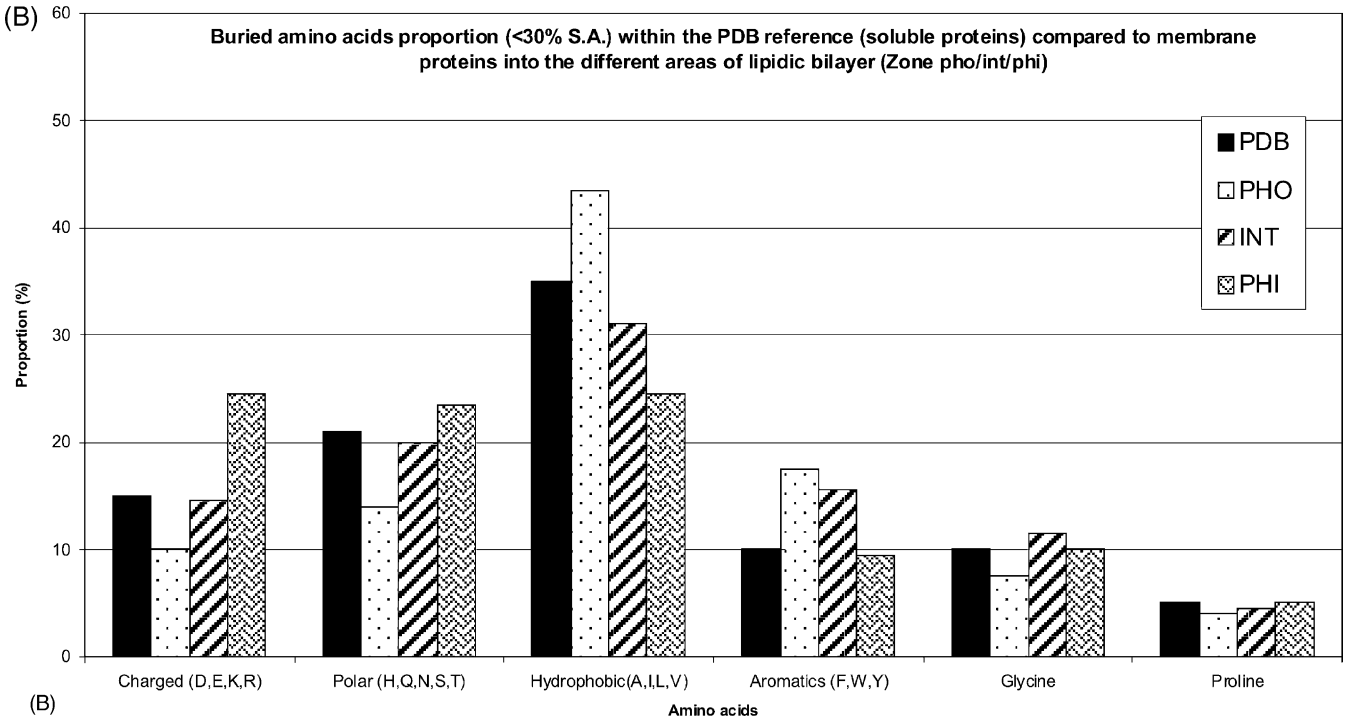

Fig. 3. (A) Plots of the frequency of accessible residues (>30% accessible surface) in a set of 131 structures of the PDB [19] as compared to a set of membrane proteins (α and β). Membrane protein residues are clustered according to the membrane zones in which they are: pho-interface-phi. Frequency of each amino acid is set as: $\left(\sum R > 30\%\,\text{S.A.Pho} / \sum \text{total residue} > 30\%\,\text{S.A.Pho}\right) \times 100$. Histograms are sorted by families of amino acids which correspond to the charged residues (D, E, K, R), polar residues (H, Q, N, S, T), hydrophobic (A, I, L, V), aromatic (F, W, Y), glycine and proline. In black are the PDB. (B) Plots of the same frequencies but for buried residues (<30% accessible surface). Columns with different hatching are the different zones (pho-interface-phi) of the bilayer as specified on the plot.

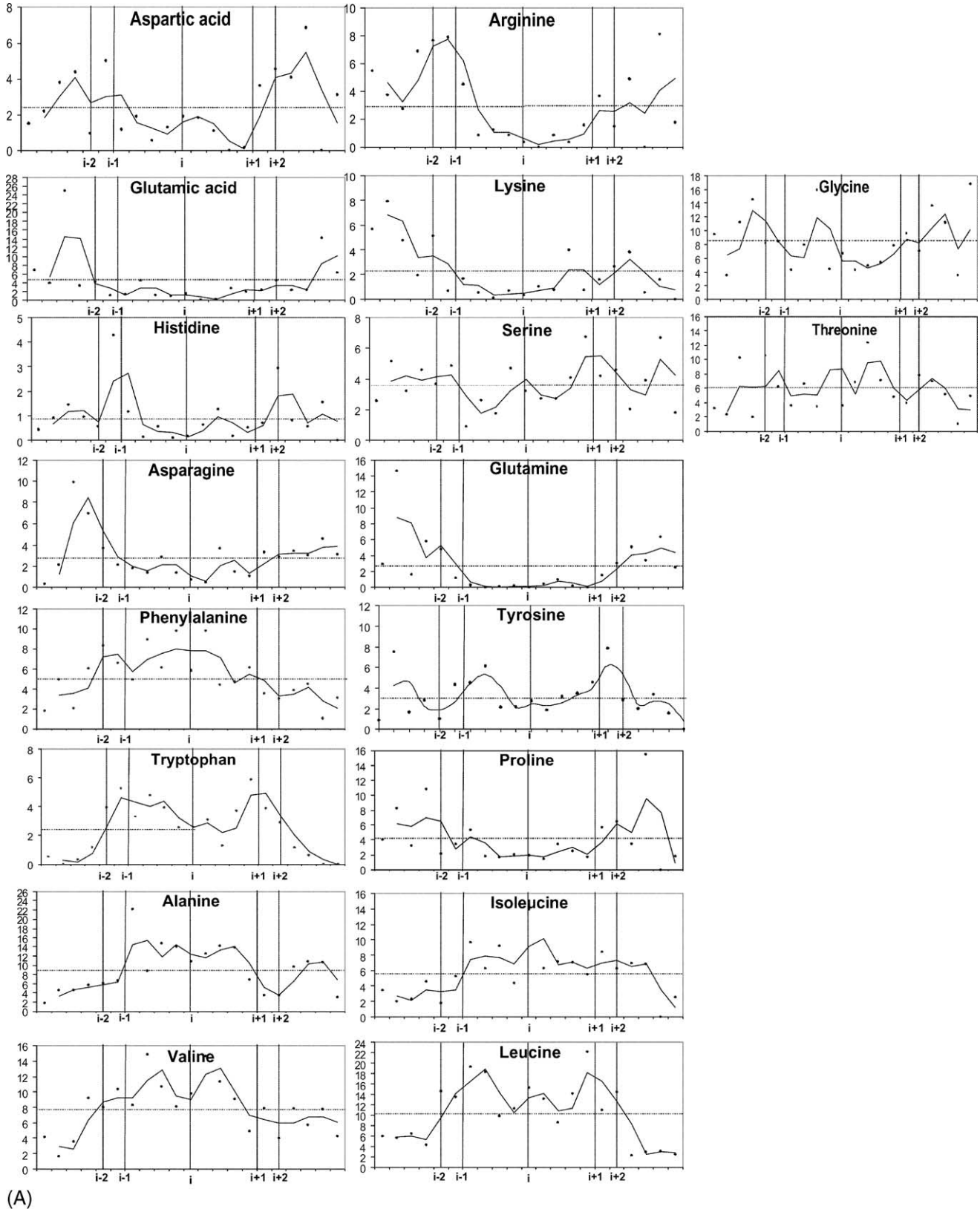

Fig. 4. The graphs show the distribution of all amino acids as the location of their C_α along the *z*-axis of the bilayer for α and β membrane proteins; *i* stands for the center of the bilayer, $i+1$ and $i-1$ for the beginning of polar heads and $i+2$ and $i-2$ for the interface polar heads–water, i.e. the end of the bilayer. Negative side represents the cytoplasmic side and positive side the extracellular one. For each graph, every point is the average frequency of a residue at one particular thickness of the bilayer for: (A) α proteins; and (B) β proteins. The lines follow the average calculated between two next points of the distribution of amino acids across the membrane.

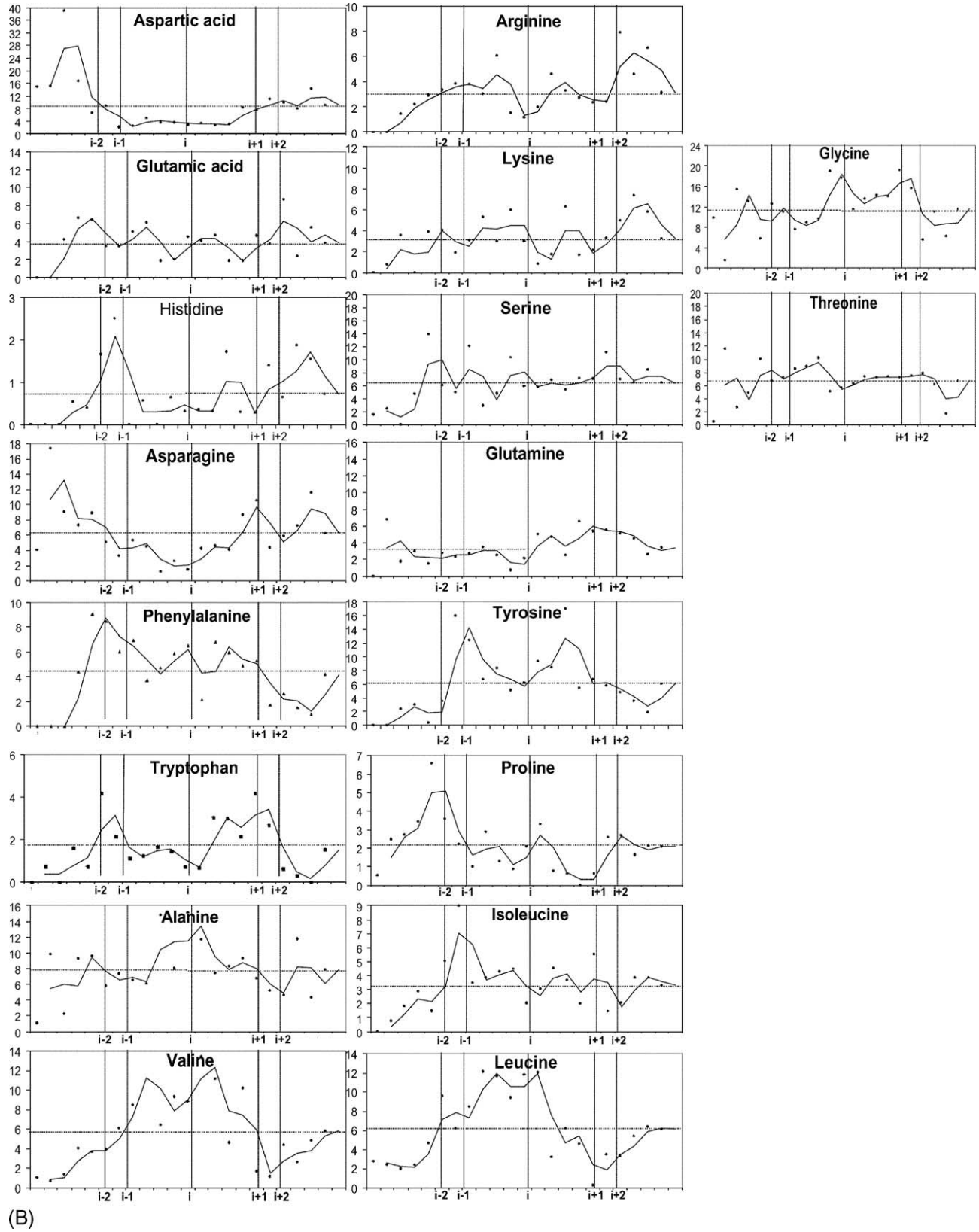

Fig. 4. (*Continued*).

arginine are mainly located outside the hydrophobic layer in α proteins and since individual examination of proteins did not reveal any special bending of side chains. However, our study has been made on rigid-body X-ray structures. One could wonder how these structures adapt when they must insert in a thicker membrane. For instance, it is unlikely that the squalene hopene cyclase can find a membrane of 21 Å thickness. However, this protein has seven lysine and 19 arginine actually located in the interface. Examination of the crystalline structure shows that the side chains are mostly perpendicular to the protein surface. Then, those residues are good candidates for stretching their side chain in order to accommodate a thicker membrane, especially if negative charges in the lipid polar head attract their amine moieties.

Polar residues: In the α proteins, histidine is more frequently found at the interface on the cytoplasmic side, and threonine and serine are dispersed along the membrane. Asparagine and glutamine are almost absent inside the membrane but are mainly found outside of the bilayer on the cytoplasmic side. For the β proteins, all the polar residue distribution patterns are similar, but asparagine occurs more often.

Hydrophobic residues: In the literature, Ulmschneider and Sansom [29] reported that the hydrophobic residues: alanine, leucine, isoleucine, phenylalanine and valine are the most frequent amino acids of transmembrane segments, accounting for about 34% of the residues in α-helical and 28% in β-barrel proteins. In α and β proteins, all hydrophobic residues are more frequent in the membrane than outside. Valine and leucine show two peaks on both sides of the membrane center. Isoleucine show a small peak at the center of the bilayer for α proteins and at the interface on the cytoplasmic side for β proteins.

Aromatic residues: In α proteins, phenylalanine is homogeneously distributed in the membrane layers. For β proteins, the frequency is higher at the interface of the cytoplasmic side. This is mostly in agreement with the literature where phenylalanine is described to be abundant in transmembrane segments [29] with a preferred location at the bilayer interface [27,30]. Tryptophan is more frequent at both the membrane interfaces. This is in agreement with the literature where tryptophan was suggested to have affinity for a well-defined site near the lipid carbonyl region [28], and to be able to inhibit protein aggregation [1]. Tyrosine is not frequent in α proteins (3% as compared to 6% in β protein) and has two peaks of frequency especially in β proteins, one at the interface on the intracellular side and another in the hydrophobic core. Tyrosine was described to anchor proteins into membranes by interacting with the lipid head groups [29].

Overall, aromatic residues were described to form a “aromatic belts” at 15 Å from the bilayer center for α-helical proteins and at 10 Å for β-barrels [29]. Tryptophan is candidate for the belt in α and β structures, tyrosine for the belt in β structures. Phenylalanine is also candidate but its distribution is also more dispersed across the bilayer. The difference between the 15 and 10 Å of the belt distance to the membrane center seems related to the optimal membrane thickness that is about 10 Å (5 Å per layer) more for α than β proteins. Those belts could be useful to identify new membrane-spanning segments from sequence databases [31].

In membrane proteins, glycine is less frequent in α than in β structures. Glycine was reported to be frequent in transmembrane segments [32], a result that we confirm for β proteins. Glycine was reported to occur at the helix–helix interfaces in membrane proteins [33] and was suggested to facilitate a close packing of transmembrane helices [34,35], a possibility that is not tested in the present analysis.

Proline is more frequent outside the membrane on the extracellular side for α proteins and on the cytoplasmic side for β proteins. In the literature, proline was described to be more frequent in loop regions, thus outside the membrane layer [36] but it was also reported to occur at the center of the membrane where it would play a structural role by modifying the conformation of transmembrane helices. Those molecular hinges might have a function in transduction of biological signal across membranes [37]. Molecular hinges do not seem to be a current role because proline of α proteins is infrequent at the membrane center.

4. Conclusions

We have looked for the optimal membrane thickness to insert 20 X-ray structures of proteins. The results demonstrate a good adequacy with previous analyses when they exist and suggest that some X-ray structure must adapt in order to insert in a biological membrane. Indeed, there is a good agreement between the 38 Å membrane in which the X-ray structure of the photosynthetic reaction center optimally inserts and the 40–45 Å thickness value obtained by a membrane–protein interaction model, where the hydrophobic energy is minimized with the energy function of Eisenberg and McLachlan [38]. There is also a good agreement between the 56 Å membrane in which the light harvesting complex II is optimally inserted and the 52.5 Å measure obtained by crystal packing in unit cell [39]. For the MsCl protein, 34 Å must be compared to the 35 Å thickness observed by cross-linking experiments and electron microscopy [40]. Interestingly, we find that the β proteins require thinner membranes than helix bundles, a finding that agrees with Rahman et al. [12] and Tamm et al. [41] who reported that bacterial membranes are made of short acyl chains.

The statistical analysis of amino acid distribution shows that many hydrophobic residues and, a few hydrophilic ones, are accessible. Aromatic residues, at least tyrosine and tryptophan, make the “aromatic belt” described in the literature, whereas phenylalanine is globally distributed within the whole bilayer. Glycine is more frequent in membranous β structures than in soluble proteins. The distribution of charged residues of α protein except glutamic acid correlate

with the positive-inside rule of von Heijne [26] who postulated that cytoplasmic segments contain more positive charge.

Our data support that most X-ray structures insert in membranes in agreement with experimental data, but a few cases could be interesting to analyze. For instance, the squalene hopene cyclase should require side chain movement in order to insert in a current membrane.

Acknowledgements

Robert Brasseur is Research Director of the National Funds For Scientific Research of Belgium (FNRS). This work was supported by the "Inter-University Poles of Attraction Programme—Belgian state, Primer Minister's office—Federal Office for Scientific, Technical and Cultural Affairs" PAI contract no. 4/03 and the work of F. Basyn was supported by a grant FNRS—Televie. O. Bouffioux was supported by the "Ministère de la region wallonne" with the PROTMEM convention (no. 14540).

References

[1] J.A. Killian, Hydrophobic mismatch between proteins and lipids in membranes, Biochim. Biophys. Acta 1376 (1998) 401–415.
[2] O.G. Mouritsen, M. Bloom, Mattress model of lipid–protein interactions in membranes, Biophys. J. 46 (1984) 141–153.
[3] J.A. Demmers, E. van Duijn, J. Haverkamp, D.V. Greathouse, R.E. Koeppe, A.J. Heck, J.A. Killian, Interfacial positioning and stability of transmembrane peptides in lipid bilayers studied by combining hydrogen–deuterium exchange and mass spectrometry, J. Biol. Chem. 276 (2001) 34501–34508.
[4] A.G. Lee, How lipids interact with an intrinsic membrane protein: the case of the calcium pump, Biochim. Biophys. Acta 1376 (1998) 381–390.
[5] N. Mobashery, C. Nielsen, O.S. Andersen, The conformational preference of gramicidin channels is a function of lipid bilayer thickness, FEBS Lett. 412 (1997) 15–20.
[6] M.A. Lemmon, D.M. Engelman, Specificity and promiscuity in membrane helix interactions, Q. Rev. Biophys. 27 (1994) 157–218.
[7] J.F. Hunt, T.N. Earnest, O. Bousche, K. Kalghatgi, K. Reilly, C. Horvath, K.J. Rothschild, D.M. Engelman, A biophysical study of integral membrane protein folding, Biochemistry 36 (1997) 15156–15176.
[8] R.M. Epand, Lipid polymorphism and protein–lipid interactions, Biochim. Biophys. Acta 1376 (1998) 353–368.
[9] S. Morein, R.E. Koeppe II, G. Lindblom, B. de Kruijff, J.A. Killian, The effect of peptide–lipid hydrophobic mismatch on the phase behavior of model membranes mimicking the lipid composition in *Escherichia coli* membranes, Biophys. J. 78 (2000) 2475–2485.
[10] E. Pedrazzini, A. Villa, N. Borgese, A mutant cytochrome b5 with a lengthened membrane anchor escapes from the endoplasmic reticulum and reaches the plasma membrane, Proc. Natl. Acad. Sci. U.S.A. 93 (1996) 4207–4212.
[11] M. Yang, J. Ellenberg, J.S. Bonifacino, A.M. Weissman, The transmembrane domain of a carboxyl-terminal anchored protein determines localization to the endoplasmic reticulum, J. Biol. Chem. 272 (1997) 1970–1975.
[12] M.M. Rahman, V.S. Kolli, C.M. Kahler, G. Shih, D.S. Stephens, R.W. Carlson, The membrane phospholipids of Neisseria meningitidis and Neisseria gonorrhoeae as characterized by fast atom bombardment mass spectrometry, Microbiology 146 (Pt 8) (2000) 1901–1911.
[13] H. Chen, D.A. Kendall, Artificial transmembrane segments: requirements for stop transfer and polypeptide orientation, J. Biol. Chem. 270 (1995) 14115–14122.
[14] L. Lins, P. Ducarme, E. Breukink, R. Brasseur, Computational study of nisin interaction with model membrane, Biochim. Biophys. Acta 1420 (1999) 111–120.
[15] P. Ducarme, M. Rahman, R. Brasseur, IMPALA: a simple restraint field to simulate the biological membrane in molecular structure studies, Proteins 30 (1998) 357–371.
[16] G. Drin, H. Demene, J. Temsamani, R. Brasseur, Translocation of the pAntp peptide and its amphipathic analogue AP-2AL, Biochemistry 40 (2001) 1824–1834.
[17] M. Lindgren, X. Gallet, U. Soomets, M. Hallbrink, E. Brakenhielm, M. Pooga, R. Brasseur, U. Langel, Translocation properties of novel cell penetrating transportan and penetratin analogues (In Process Citation), Bioconjug. Chem. 11 (2000) 619–626.
[18] F. Basyn, B. Charloteaux, A. Thomas, R. Brasseur, Prediction of membrane protein orientation in lipid bilayers: a theoretical approach, J. Mol. Graph. Model. 20 (2001) 235–244.
[19] A. Thomas, O. Bouffioux, D. Geeurickx, R. Brasseur, Pex, analytical tools for PDB files. Part I. GF-Pex: basic file to describe a protein, Proteins 43 (2001) 28–36.
[20] D.A. Doyle, C.J. Morais, R.A. Pfuetzner, A. Kuo, J.M. Gulbis, S.L. Cohen, B.T. Chait, R. MacKinnon, The structure of the potassium channel: molecular basis of K^+ conduction and selectivity (see comments), Science 280 (1998) 69–77.
[21] J. Vogt, G.E. Schulz, The structure of the outer membrane protein OmpX from *Escherichia coli* reveals possible mechanisms of virulence, Structure. Fold. Des. 7 (1999) 1301–1309.
[22] E. Sim, Membrane Biochemistry, Chapman and Hall Ltd., London, 1982.
[23] H. Heller, M. Schaefer, K. Schulten, Molecular dynamics simulation of a bilayer of 200 lipids in the gel and in the liquid–crystal phases, J. Phys. Chem. 97 (2002) 8343–8360.
[24] J.H. Kleinschmidt, L.K. Tamm, Secondary and tertiary structure formation of the β-barrel membrane protein OmpA is synchronized and depends on membrane thickness, J. Mol. Biol. 324 (2002) 319–330.
[25] T.E. Creighton, Proteins: Structures and Molecular Properties, 2nd ed., Freeman, New York, 1993.
[26] G. von Heijne, Membrane protein structure prediction: hydrophobicity analysis and the positive-inside rule, J. Mol. Biol. 225 (1992) 487–494.
[27] J.A. Killian, G. von Heijne, How proteins adapt to a membrane–water interface, Trends Biochem. Sci. 25 (2000) 429–434.
[28] M.R. de Planque, J.A. Kruijtzer, R.M. Liskamp, D. Marsh, D.V. Greathouse, R.E. Koeppe, B. de Kruijff, J.A. Killian, Different membrane anchoring positions of tryptophan and lysine in synthetic transmembrane α-helical peptides, J. Biol. Chem. 274 (1999) 20839–20846.
[29] M.B. Ulmschneider, M.S. Sansom, Amino acid distributions in integral membrane protein structures, Biochim. Biophys. Acta 1512 (2001) 1–14.
[30] S. Persson, J.A. Killian, G. Lindblom, Molecular ordering of interfacially localized tryptophan analogs in ester– and ether–lipid bilayers studied by ^{2}H NMR, Biophys. J. 75 (1998) 1365–1371.
[31] W.C. Wimley, Toward genomic identification of β-barrel membrane proteins: composition and architecture of known structures, Protein Sci. 11 (2002) 301–312.
[32] C. Landolt-Marticorena, K.A. Williams, C.M. Deber, R.A. Reithmeier, Non-random distribution of amino acids in the transmembrane segments of human type I single span membrane proteins, J. Mol. Biol. 229 (1993) 602–608.
[33] M.M. Javadpour, M. Eilers, M. Groesbeek, S.O. Smith, Helix packing in polytopic membrane proteins: role of glycine in transmembrane helix association, Biophys. J. 77 (1999) 1609–1618.

[34] M. Eilers, S.C. Shekar, T. Shieh, S.O. Smith, P.J. Fleming, Internal packing of helical membrane proteins, Proc. Natl. Acad. Sci. U.S.A. 97 (2000) 5796–5801.
[35] A. Senes, I. Ubarretxena-Belandia, D.M. Engelman, The C_αH–O hydrogen bond: a determinant of stability and specificity in transmembrane helix interactions, Proc. Natl. Acad. Sci. U.S.A. 98 (2001) 9056–9061.
[36] E. Wallin, T. Tsukihara, S. Yoshikawa, G. von Heijne, A. Elofsson, Architecture of helix bundle membrane proteins: an analysis of cytochrome c oxidase from bovine mitochondria, Protein Sci. 6 (1997) 808–815.
[37] M.S. Sansom, H. Weinstein, Hinges, swivels and switches: the role of prolines in signaling via transmembrane α-helices, Trends Pharmacol. Sci. 21 (2000) 445–451.
[38] T.O. Yeates, H. Komiya, D.C. Rees, J.P. Allen, G. Feher, Structure of the reaction center from *Rhodobacter sphaeroides* R-26: membrane–protein interactions, Proc. Natl. Acad. Sci. U.S.A. 84 (1987) 6438–6442.
[39] J. Koepke, X. Hu, C. Muenke, K. Schulten, H. Michel, The crystal structure of the light-harvesting complex II (B800-850) from *Rhodospirillum molischianum*, Structure 4 (1996) 581–597.
[40] G. Chang, R.H. Spencer, A.T. Lee, M.T. Barclay, D.C. Rees, Structure of the MscL homolog from *Mycobacterium tuberculosis*: a gated mechanosensitive ion channel, Science 282 (1998) 2220–2226.
[41] L.K. Tamm, A. Arora, J.H. Kleinschmidt, Structure and assembly of β-barrel membrane proteins, J. Biol. Chem. 276 (2001) 32399–32402.
[42] A. Villarroel, O. Alvarez, A. Oberhauser, R. Latorre, Probing a Ca^{2+}-activated K^+ channel with quaternary ammonium ions, Pflugers Arch. 413 (1988) 118–126.
[43] I. Koltover, J.O. Raedler, T. Salditt, K.J. Rothschild, C.R. Safinya, Phase behavior and interactions of the membrane–protein bacteriorhodopsin, Am. Phys. Soc. 82 (2001) 3184–3187.
[44] S.A. Verclas, P.B. Howes, K. Kjaer, A. Wurlitzer, M. Weygand, G. Buldt, N.A. Dencher, M. Losche, X-ray diffraction from a single layer of purple membrane at the air–water interface, J. Mol. Biol. 287 (1999) 837–843.
[45] S. Tristram-Nagle, C.P. Yang, J.F. Nagle, Thermodynamic studies of purple membrane, Biochim. Biophys. Acta 854 (1986) 58–66.
[46] R.M. Glaeser, T.A. Ceska, High-voltage electron diffraction from bacteriorhodopsin (purple membrane) is measurably dynamical, Acta Crystallogr. A 45 (Pt 9) (1989) 620–628.
[47] D. Forst, W. Welte, T. Wacker, K. Diederichs, Structure of the sucrose-specific porin ScrY from *Salmonella typhimurium* and its complex with sucrose (see comments), Nat. Struct. Biol. 5 (1998) 37–46.
[48] A.D. Ferguson, E. Hofmann, J.W. Coulton, K. Diederichs, W. Welte, Siderophore-mediated iron transport: crystal structure of FhuA with bound lipopolysaccharide (see comments), Science 282 (1998) 2215–2220.
[49] E.J. Boekema, M. Stuart, R.I. Koning, W. Keegstra, A. Brisson, H.M. Verheij, N. Dekker, A 7.4-Å projection structure of outer membrane phospholipase A from *Escherichia coli* by electron crystallography, J. Struct. Biol. 123 (1998) 67–71.